Approximation of the acoustic and elastic wave equations by generalized finite difference stencils applied the unstructured grids.

Juliano D. B. Santos[1], Abimael F. D. Loula[1], Geraldo J. B. dos Santos[2]

[1]*Laboratório Nacional de Computação Científica*
Av. Getúlio Vargas, 333 – Petrópolis-RJ – CEP: 25.651-075 – Brasil
juliano@lncc.br, aloc@lncc.br
[2]*Department of Technology, State University of Feira de Santana*
Avenida Transnordestina, s/n - Novo Horizonte- CEP 44036-900 - Ba - Brasil
belmonte@uefs.br

Abstract. Classical finite difference methodologies, obtained through Taylor series expansions of the functions, are feasible only when the points are distributed on structured or Cartesian grids defined over rectangular domains or mapped to rectangles. In this paper we present a technique capable of generating approximations for the two-dimensional acoustic and elastic wave equations on structured and unstructured meshes over more general domains. The stencils were calculated at each point of the arbitrary grid by interpolation techniques and the results shown that the order of accuracy, obtained when the structured grid is used, is maintain to case unstructured and minimum number of points of the stencils.

Keywords: Unstructured meshes, Finite difference, Wave equation

1 Introduction

A paper that introduced finite difference discretizations in transient problems was [1], where Maxwell's equations of electromagnetism are approximated on interleaved meshes, which can be understood as a dual mesh containing points of a discrete finite difference mesh and an intermediate mesh, where the classical finite difference operators are obtained at the points of the original mesh by means of approximations performed on an intermediate mesh. Generalized finite difference methods (GFDM) presented in [2] made it possible to simulate applied mechanics problems on more general domains and irregular meshes, where approximations for elliptic and parabolic problems are obtained by the method of least squares. In [3] the finite difference approximations on intercalated meshes introduced in the work of Kane Yee [1] are used in modeling seismic wave propagation problems. In what follows, the GFDM was extended in [4] where hyperbolic partial differential equations are also studied.

2 Transient wave equations

Let $\Omega \subset \mathbb{R}^2$ be a smooth subset and $[0, T]$ be a time interval. The model problem with source term associated with the acoustic wave equation will be defined as

$$\frac{\partial^2 u}{\partial t^2} - \nabla \cdot (c^2 \nabla u) = f(x, y, t) \text{ on } \Omega \times (0, T), \tag{1}$$

$$u(., t) = 0 \text{ on } \partial\Omega \times (0, T), \tag{2}$$

$$u(., 0) = u_0, \;\; u_t(., 0) = v_0 \text{ on } \Omega. \tag{3}$$

with c constant.

The mathematical model capable of describing the propagation of elastic waves given a vectorial field $\boldsymbol{u}(u_1, u_2)$ that satisfies it, under these conditions, is given by

$$\begin{cases} \rho \dfrac{\partial^2 \boldsymbol{u}}{\partial t^2} & -\mathrm{div}\boldsymbol{\sigma}(\boldsymbol{u}) = \boldsymbol{f}, \ \text{ on } \Omega, \\ & \boldsymbol{\sigma}(\boldsymbol{u}) = \mathbb{D}\boldsymbol{\varepsilon}(\boldsymbol{u}) \ \text{ on } \ \Omega, \\ & \boldsymbol{u} = \boldsymbol{0} \ \text{ on } \Gamma, \end{cases} \tag{4}$$

subject to initial conditions

$$\boldsymbol{u}(\boldsymbol{x}, \boldsymbol{0}) = \boldsymbol{u_0}(\boldsymbol{x}), \ \frac{\partial \boldsymbol{u}(\boldsymbol{x}, \boldsymbol{0})}{\partial t} = \boldsymbol{v_0}(\boldsymbol{x}), \tag{5}$$

where $u_i = u_i(x_1, x_2, t)$, $i = 1, 2$, represent the displacements of the solid oriented by the directions x_1 and x_2, in that order.

Here the ρ parameter is the density of the medium, which we will adopt as constant, $\boldsymbol{\sigma} = [\boldsymbol{\sigma}_1, \boldsymbol{\sigma}_2]$ is the symmetric Cauchy stress tensor, $\mathbb{D} = 2\mu\mathbb{I} + \lambda \boldsymbol{I} \otimes \boldsymbol{I}$ is the isotropic elasticity tensor where $\boldsymbol{I}$is the second-order identity tensor and $\mathbb{I}$ is the fourth-order identity tensor on symmetric second-order tensors. The linear strain tensor is defined as $\boldsymbol{\varepsilon}(\boldsymbol{u}) = \frac{1}{2}(\nabla \boldsymbol{u} + \nabla \boldsymbol{u}^T)$. Furthermore, the symmetric strain tensor can be defined, under these media conditions, as a function of the constitutive parameters. That is, the functions defining the stress vector $\boldsymbol{\sigma}_i := [\sigma_{i1}, \sigma_{i2}]^T$, $i = 1, 2$ can therefore be written in terms of the constitutive parameters

$$\boldsymbol{\sigma}_1 = \begin{pmatrix} (2\mu + \lambda)\frac{\partial u_1}{\partial x_1} + \lambda \frac{\partial u_2}{\partial x_2} \\ \mu \left(\frac{\partial u_1}{\partial x_2} + \frac{\partial u_2}{\partial x_1} \right) \end{pmatrix}, \boldsymbol{\sigma}_2 = \begin{pmatrix} \mu \left(\frac{\partial u_1}{\partial x_2} + \frac{\partial u_2}{\partial x_1} \right) \\ \lambda \frac{\partial u_1}{\partial x_1} + (2\mu + \lambda)\frac{\partial u_2}{\partial x_2} \end{pmatrix}. \tag{6}$$

where μ and λ are the Lamé coefficients. For plane and linear stresses the Lamé coefficients are given by the relations

$$\lambda = \frac{E\upsilon}{(1+\upsilon)(1-2\upsilon)}, \ \ \mu = \frac{E}{2(1+\upsilon)}, \tag{7}$$

where E and υ are the modulus of elasticity and Poisson's ratio, respectively.

We cite [5, 6] and [7, 8], in that order, as example articles where classical operator approximations are presented for the acoustic and elastic wave equations.

3 Approximations of operators on unstructured meshes

Obtaining approximations for differential operators can be accomplished by defining stencils and calculating their coefficients. The mathematical model of a generic boundary value problem can be abstractly presented as:
Finding a function $\mathbf{u}(\mathrm{x})$***:*** $\Omega \longrightarrow \mathbb{R}^{n_{sd}}$, $\forall \mathrm{x} \in \Omega$***, so that***

$$\begin{cases} \mathcal{L}(\mathbf{u}) = \mathbf{f} & \text{on } \Omega, \\ \\ \mathcal{B}(\mathbf{u}) = \bar{\mathbf{g}} & \text{over } \partial\Omega, \end{cases} \tag{8}$$

where $\mathcal{L}$ denotes a differential operator, $\mathbf{f}$ is the source term and $\mathcal{B}$ a condition on the $\partial\Omega$ edge of the domain. In particular, the spatial differential operators associated with the equations (1) and (4), in that order, will be

$$\mathcal{L} := \frac{\partial^2}{\partial x^2} + \frac{\partial^2}{\partial y^2} \tag{9}$$

and

$$\mathcal{L} := \mathrm{div}\boldsymbol{\sigma}(\ \ ). \tag{10}$$

The methodology to discretize the equations obtained by the (9) and (10) operators will be feasible for stencils with arbitrary amounts of points, distributed on uniform or non-uniform meshes. In the following we will rely on the abstract notations for mesh, points and stencils presented in [9, 10].

Let X be a finite set such that $|X|$ denote its number of elements and $\mathcal{N} = \{\mathbf{x}_0, \ldots, \mathbf{x}_{|\mathcal{N}|-1}\} \subset \Omega \cup \Gamma$ a set of indexed points, also called nodes, where the solution can be evaluated and approximated. We will denote the set of points as $\mathcal{N}$ on the inside of Ω by $\mathcal{I}$, so that $\mathcal{I} := \mathcal{N} \cap \Omega$. The set of $\mathcal{N}$ on the Ω boundary will be denoted by $\mathcal{BP} := \mathcal{N} \cap \Gamma$. In addition, for each $i \in \{0, \ldots, |\mathcal{N}| - 1\}$, will be associated with the set $\mathcal{A}_i \subset \{0, \ldots, |\mathcal{N}| - 1\}$, which contains the points adjacent to x_i chosen by a certain criterion. Thus, if $j \in \mathcal{A}_i$, we have that x_j is adjacent to x_i. For the applications that will be made later it will be enough for us to admit that $i \in \mathcal{A}_i$, for all $i \in \{0, \ldots, |\mathcal{N}| - 1\}$.

Being $\mathbf{x}$ a given point in $\mathcal{N}$, we associate an index ind($\mathbf{x}$), that for any $i \in \{0, \ldots, |\mathcal{N}| - 1\}$, is given by $\text{ind}(\mathbf{x}_i) := i$. It follows that $\text{ind}(X)$ will be the set of indices of the points of X in $\mathcal{N}$. In particular, we have that $\text{ind}(\mathcal{N}) = \{0, \ldots, |\mathcal{N}| - 1\}$.

Considering that the equation (8) is a partial differential equation of one scalar variable $u(\mathbf{x})$, its classical finite-difference approximation over a point $\mathbf{x}_i \in \mathcal{I}$ must meet the following relation

$$\mathcal{L}u(\mathbf{x}_i) \cong \sum_{j \in \mathcal{A}_i} c_j u(\mathbf{x}_j), \tag{11}$$

with the coefficients c_j, with $j \in \mathcal{A}_i$, calculated such that the value of the operator $\mathcal{L}$ on the variable u at the point $\mathbf{x}_i$ is given as a linear combination of the values of the function u evaluated at points $\mathbf{x}_j$ belonging to a neighborhood $\mathcal{A}_i$ of $\mathbf{x}_i$. The operator approximation will be characterized by the coefficients c_j of the stencil (11). Classically these coefficients are obtained by Taylor series developments.

In our approach obtaining the coefficients c_j of the finite difference stencil centered at $\mathbf{x}_i$, in the direct expression (11), is feasible by replacing the variable u by m functions to be chosen from a set $\mathbb{B}_i$ and evaluated at the point $\mathbf{x}_i$. Equivalently, through a $\mathbb{B}_i$ basis with m functions φ_l,

$$\mathbb{B}_i := \{\varphi_1, \varphi_2, \ldots, \varphi_m\}, \tag{12}$$

we obtain for each φ_l, $l = 1, \ldots, m$, an equation,

$$\sum_{j \in \mathcal{A}_i} c_j \varphi_l(\mathbf{x}_j) = \mathcal{L}\varphi_l(\mathbf{x}_i), \tag{13}$$

which is evaluated at the point $\mathbf{x}_i$, resulting in a system of m linear algebraic equations and $|\mathcal{A}_i|$ unknowns c_j, more details in [10].

If we consider that the functions of the set $\mathbb{B}_i$ on (12) are canonical polynomials in two-dimensional space and in coupled time such as

$$\mathbb{B} := \{1, x, y, x^2, y^2, xy, x^2y, xy^2, x^2y^2\}. \tag{14}$$

we extend our result presented in [11] to a 2D domain, so that the system of algebraic equations generated by the proposed approximation method for finite differences on non-uniform meshes will be given by

$$\frac{\mathbf{U^{n+1}} - 2\mathbf{U^n} + \mathbf{U^{n-1}}}{\Delta t^2} + \mathbf{K}\mathbf{U^n} = \mathbf{F^n}, \tag{15}$$

where $\mathbf{U^n}$ is the vector of nodal unknowns and $\mathbf{K}$ is the stiffness matrix associated with the discretization of the Laplacian operator. From (15) we explicitly obtain

$$\mathbf{U^{n+1}} = 2\mathbf{U^n} - \mathbf{U^{n-1}} + \Delta t \left(\mathbf{F^n} - \mathbf{K}\mathbf{U^n}\right) \tag{16}$$

as a consequence of the fact that in these difference approximations the mass matrix remains diagonal because, in time, classical second order discretizations will be adopted in all cases. Moreover, the discrete equation (16) is an extension to the two-dimensional case of part of the results presented in [11].

4 Structure of meshes and stencils

Figure (1) contains examples of uniform and unstructured media and meshes to be used in future experiments. As can be seen these are typical finite element meshes $\mathbb{Q}_2$. Thus, we illustrate the possibilities for spatial stencils in Figure (2).

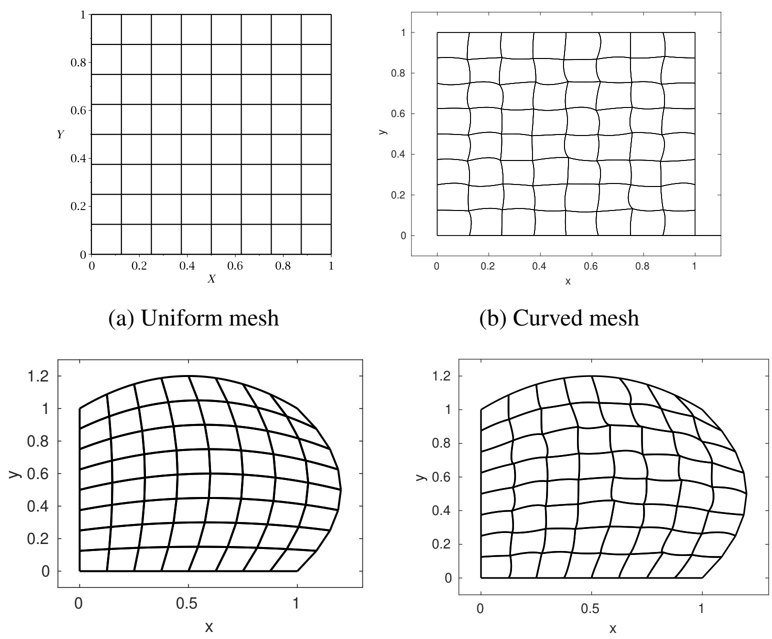

(a) Uniform mesh (b) Curved mesh

(c) Curved domain I (d) Curved domain II

Figure 1. Sequences of point meshes, from left to right: Uniform mesh (a), Curved mesh (b), Curved mesh/domain (c)-(d).

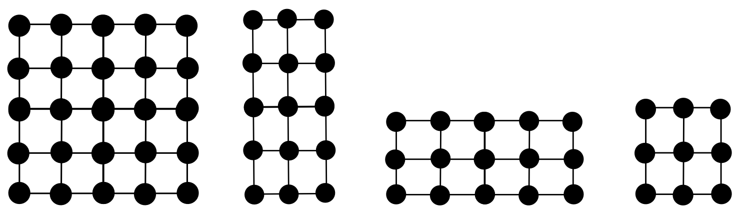

(a) (b) (c) (d)

Figure 2. Structure of the stencils.

For 9-point space stecils(Figure (2d)) the set of monomials is obtained by the product of the spaces of functions

$$\mathbb{B}_9 = \{(1, x, x^2) \otimes (1, y, y^2)\}. \tag{17}$$

The 15-point stencils (Figures (2b) and (2c)) contemplate two situations, namely,

$$\mathbb{B}_{15} := \{(1, x, x^2, x^3, x^4) \otimes (1, y, y^2)\} \text{ or } \mathbb{B}_{15} =: \{(1, x, x^2) \otimes (1, y, y^2, y^3, y^4)\}. \tag{18}$$

The 25-point stencils (Figure (2a)), on the other hand, will be obtained by using the

$$\mathbb{B}_{25} := \{(1, x, x^2, x^3, x^4) \otimes (1, y, y^2, y^3, y^4)\}. \tag{19}$$

When the interior coordinates are randomly perturbed it is possible for non-convex stencils to appear on the mesh. An isoparametric transformation [12] will, in some cases, lead to stencils of non-convex geometry, where the associated interpolation functions will be quadratic, resulting in second-order approximations to the interpolant in the experiments and consequent loss of optimal rate.

5 Numerical experiments

Approximations of the model problem (8) will be made on uniform and non-uniform meshes of $2^i + 1$ we, $i \in \{1, 2, 3, \ldots, 7\}$, where the wave speed was set constant $c = 1$. Adotaremos parâmetros de malha $h_i = 2^{-i}$

and time step $\Delta t = h_i/20$. The final time adopted in the experiments will be $Tf := 1$. Approximations will be made for the analytical solutions presented in Table (1).

Solution $u(x, y, t)$	Source $f(x, y, t)$
$t^2 \sin(\pi x)\sin(\pi y)$	$2\sin(\pi x)\sin(\pi y)(1 + \pi^2 t^2)$
$\cos(\sqrt{2}\pi t)\sin(\pi x)\sin(\pi y)$	0

Table 1. Analytical solutions and associated source terms.

The calculation of the error committed in approximations will be performed in the L^2 norm $\|\cdot\|$, semi-norm $\|\nabla\cdot\|$ of H^1, in addition to the well-known maximal $|\cdot|_\infty$ norm. Third-order optimal rates in L^2 for the interpolant u_i and second-order rates in the $\|\nabla\cdot\|$ semi-norm are expected in uniform mesh sequences. Concerning the approximate solution u_h suboptimal second-order rates are expected in the norms in L^2 and of the maximum because, asymptotically, the second-order truncation error of the stencils (2d), (2b) and (2c) will predominate. For the semi-norm of H^1 second-order methods must be obtained because the approximation is reconstructed inside the stencil via the nodal values of the gradient of a second-order interpolant.

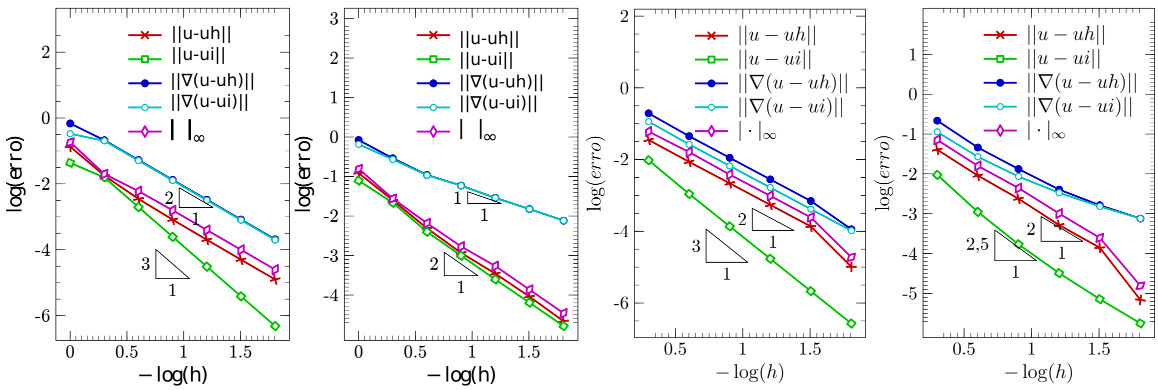

(a) Uniform mesh (b) Curved mesh (c) Domínio curvo I (d) Curved domain II

Figure 3. Errors in the convergence study h for the solution $t^2 \sin(\pi x)\sin(\pi y)$ on uniform and curved mesh sequences (a)-(b) and curved domain in the plane wave approximation $\cos(\sqrt{2}\pi t)\sin(\pi x)\sin(\pi y)$ (c)-(d).

Over a sequence of uniform meshes suboptimal rates are obtained for the approximation errors associated with the exact solution in time $t^2 \sin(\pi x)\sin(\pi y)$ (Graphic (3a)) in both norms L^2 and $|\cdot|_\infty$ because the second-order spatial error of stencils on the domain boundary defines the approximation order of the method. In addition, optimal rates in the seminorm H^1 for the approximation and interpolant are observed. For randomly deformed meshes(Graph (3b)) there is loss of optimal rate of the interpolant in addition to loss of accuracy in both norms studied as well as in the seminorm H^1.

Convergence studies performed with the refinement of type I curved domains obtained by approximating the solution $\cos(\sqrt{2}\pi t)\sin(\pi x)\sin(\pi y)$ are illustrated in Figure (3c). The interpolant u_i maintains optimal rate and expected second order behavior is verified in L^2, H^1 also in the norm of maximum. For studies with meshes over domain type II it follows that the interpolant exhibits suboptimal rate and the semi-norm of H^1 is not shown to be robust with the current mesh distortion, not having satisfactory behavior on more refined meshes.

6 Conclusions

We have presented in this work, so far, a methodology capable of generating approximations for the Laplacian space operator associated with the acoustic wave equation. The associated stencils are obtained by using independent monomials in the real variables x and y. Convergence studies on the norms in L^2 and of the maximum showed robustness for the varied mesh types and domains, with expected rates obtained. The seminorm of H^1, on the other hand, proved unable to maintain expected rates for the type II curved domain. We are developing the approximations associated with the elastic wave equation.

Acknowledgements. The authors thank CAPES, Coordenação de Aperfeiçoamento de Pessoal de Nível Superior, for the financial support to the development of this work.

Authorship statement. The authors hereby confirm that they are the sole liable persons responsible for the authorship of this work, and that all material that has been herein included as part of the present paper is either the property (and authorship) of the authors, or has the permission of the owners to be included here.

References

[1] K. Yee. Numerical solution of initial boundary value problems involving maxwell's equations in isotropic media. *IEEE Transactions on antennas and propagation*, vol. 14, n. 3, pp. 302–307, 1966.

[2] T. Liszka and J. Orkisz. The finite difference method ar arbitrary irregular grids ans its application in applied mechanics. *Computer e Structures*, , n. 11, pp. 83–95, 1980.

[3] A. R. Levander. Finite-difference forward modeling in seismology. *Geophysics*, pp. 410–431, 1989.

[4] J. Benito, F. Urena, and L. Gavete. Solving parabolic and hyperbolic equations by the generalized finite difference method. *Journal of computational and applied mathematics*, vol. 209, n. 2, pp. 208–233, 2007.

[5] J. Strikwerda. *Finite difference schemes and partial differential equations*. SIAM: Society for Industrial and Applied Mathematics, 2 edition, 2004.

[6] R. J. LeVeque. *Finite Difference Methods for Differential Equations*. University of Washington, 2005.

[7] K. R. Kelly, R. W. Ward, S. Treitel, and R. M. Alford. Synthetic seismograms: A finite-difference approach. *Geophysics*, vol. 41, n. 1, pp. 2–27, 1976.

[8] S. Nilsson, N. A. Petersson, B. Sjögreen, and H.-O. Kreiss. Stable difference approximations for the elastic wave equation in second order formulation. *SIAM Journal on Numerical Analysis*, vol. 45, n. 5, pp. 1902–1936, 2007.

[9] D. T. Fernandes. *Métodos de elementos finitos e diferenças finitas estabilizados para o problema de Helmholtz*. Tese de doutorado, LNCC, 2009.

[10] J. D. B. Santos, A. F. D. Loula, and G. J. B. Santos. Geração de aproximações de diferenças finitas em malhas não-uniformes para as edps de laplace e helmholtz. *Proceedings of the of the Brazilian Society of Computational and Applied Mathematics-CNMAC*, 2016.

[11] J. D. B. Santos and A. F. D. Loula. High-order methods for the acoustic wave equation in one space dimension. *Proceedings of the XXXVIII Iberian Latin-American Congress on Computational Methods in Engineering*, 2017.

[12] T. J. R. Hughes. *The Finite Element Method: Linear Static and Dynamic Finite Element Analysis*. Dover Civil and Mechanical Engineering. Dover Publications, 2000.